Cell Reports, Volume *43*

Supplemental information

Macrophages enhance contractile force in iPSC-derived human engineered cardiac tissue

Roberta I. Lock, Pamela L. Graney, Daniel Naveed Tavakol, Trevor R. Nash, Youngbin Kim, Eloy Sanchez Jr., Margaretha Morsink, Derek Ning, Connie Chen, Sharon Fleischer, Ilaria Baldassarri, and Gordana Vunjak-Novakovic

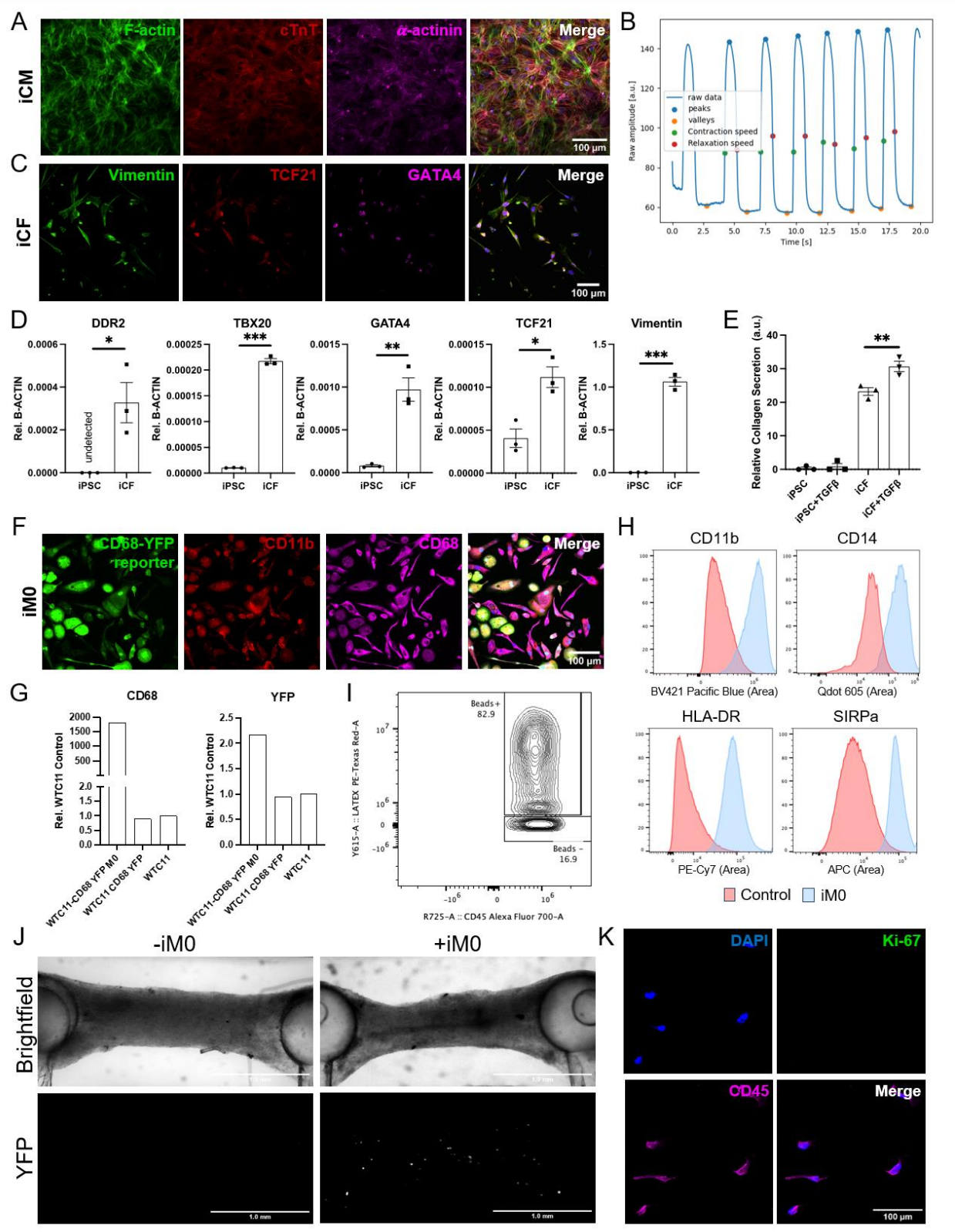

Fig. S1. Supporting data characterizing iPSC-derived cardiomyocytes, cardiac fibroblasts, and macrophages, Related to Figure 1. (A) Immunofluorescence of cardiomyocyte markers F-

actin, cTnT, and α-actinin. Scale bar = 100 μm. **(B)** Spontaneous contraction profile of iCM. **(C)** Immunofluorescence of fibroblast markers Vimentin, TCF21, and GATA4. Scale bar = 100 μm. **(D)** RT-qPCR analysis of iCF for a panel of fibroblast-specific markers. **(E)** Collagen secretion by undifferentiated iPSC and iCF in response to TGFβ stimulation, confirming iCF functionality. **(F)** Immunofluorescence of macrophage markers CD68-YFP reporter, CD11b, and CD68. Scale bar = 100 μm. **(G)** RT-qPCR analysis confirming stable expression of CD68-YFP reporter in iPSC-derived macrophages, compared to WTC11 CD68-YFP reporter and unmodified WTC11 controls. **(H)** Surface marker expression of macrophage markers in differentiated iM0 and undifferentiated WTC11 control. **(I)** Uptake of latex beads, confirming functionality of iM0. **(J)** Live cell brightfield and fluorescence imaging of hECT prepared in the absence (-iM0) and presence (+iM0) of macrophages expressing CD68-YFP. Scale bar = 1mm **(K)** Immunofluorescence of macrophage expression of CD45 for immune identity and Ki-67 as an indicator of proliferative status. Scale bar = 100 μm.

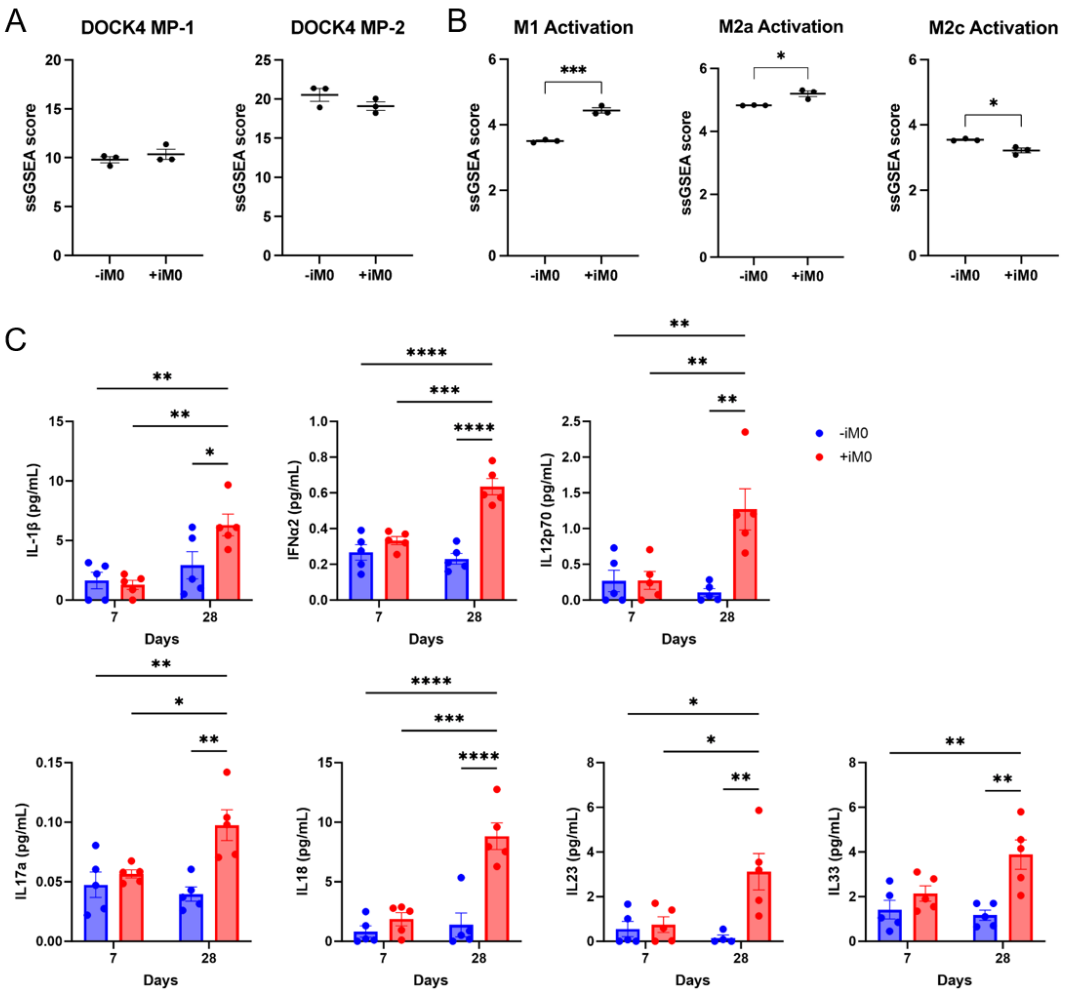

Fig. S2. Supporting data characterizing iM0 behavior in cardiac tissues, Related to Figure 2. Single sample gene set enrichment analysis (ssGSEA) for supplemental gene sets describing **(A)** macrophage populations found within the adult human heart and (**B)** human primary monocyte-derived M1, M2a, and M2c macrophage phenotypes generated in vitro. Analysis was not restricted to only differentially expressed genes. Data were analyzed via two-tailed t test. **(C)** Production by +iM0 and -iM0 hECTs of additional inflammatory cytokines in tissue supernatant after 7 and 28 days. Statistical significance was determined by two-way ANOVA with Tukey's post hoc analysis. All data represent mean ± SEM. *p<0.05, **p<0.01, ***p<0.001, **** p<0.0001.

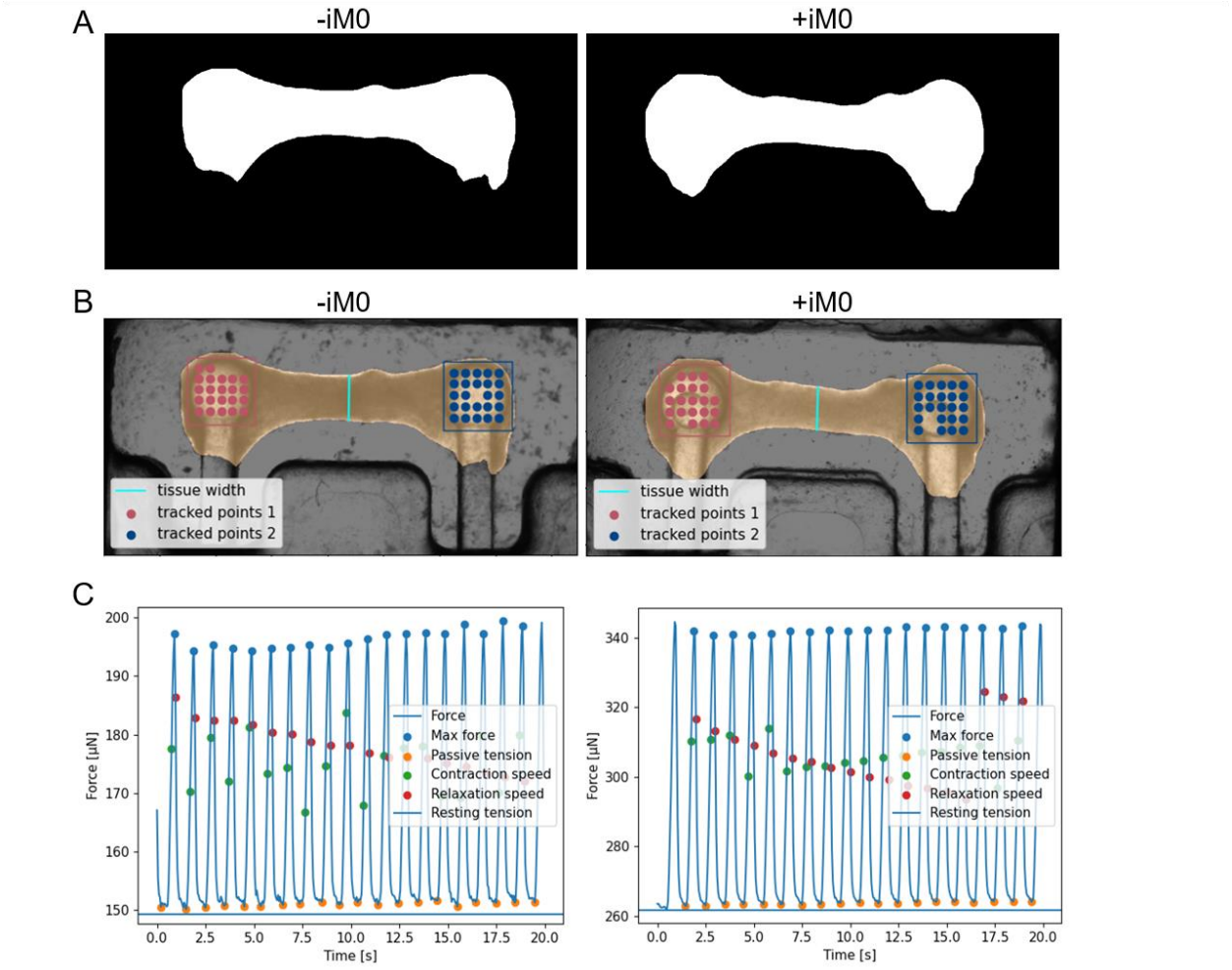

Fig. S3. Tracking and analysis of flexible pillar displacement, Related to Figure 3. (A) Image processing showing binarized identification of tissue morphology, used to identify tissue size and cross-sectional area. **(B)** Identification of pillar-heads which are tracked to measure pillar displacement for contractile function analysis. **(C)** Representative traces of contractile force generated from tracking pillar displacement that the metrics of contractility are extracted from, including maximum force, passive tension, contraction and relaxation speed, and resting tension.

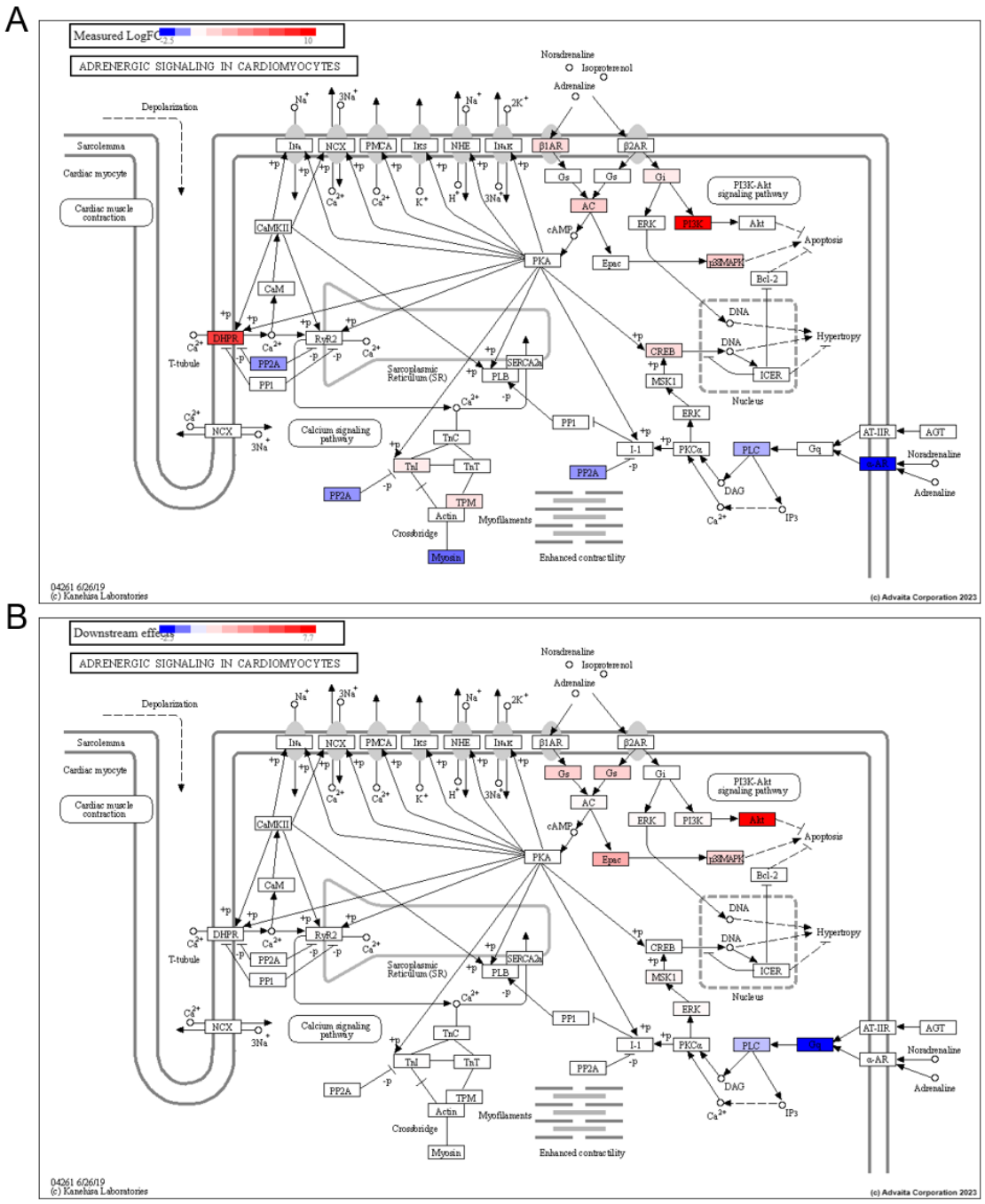

Fig. S4. Supporting KEGG pathway diagrams, Related to Figure 4. (A) KEGG Pathway Diagram of Adrenergic signaling in cardiomyocytes showing measured expression of differentially expressed genes from the RNA-sequencing dataset. **(B)** KEGG Pathway Diagram of Adrenergic signaling in cardiomyocytes, showing computed accumulated perturbation across pathway topology from differentially expressed upstream genes. Diagrams were generated using AdvaitaBio iPathwayGuide.

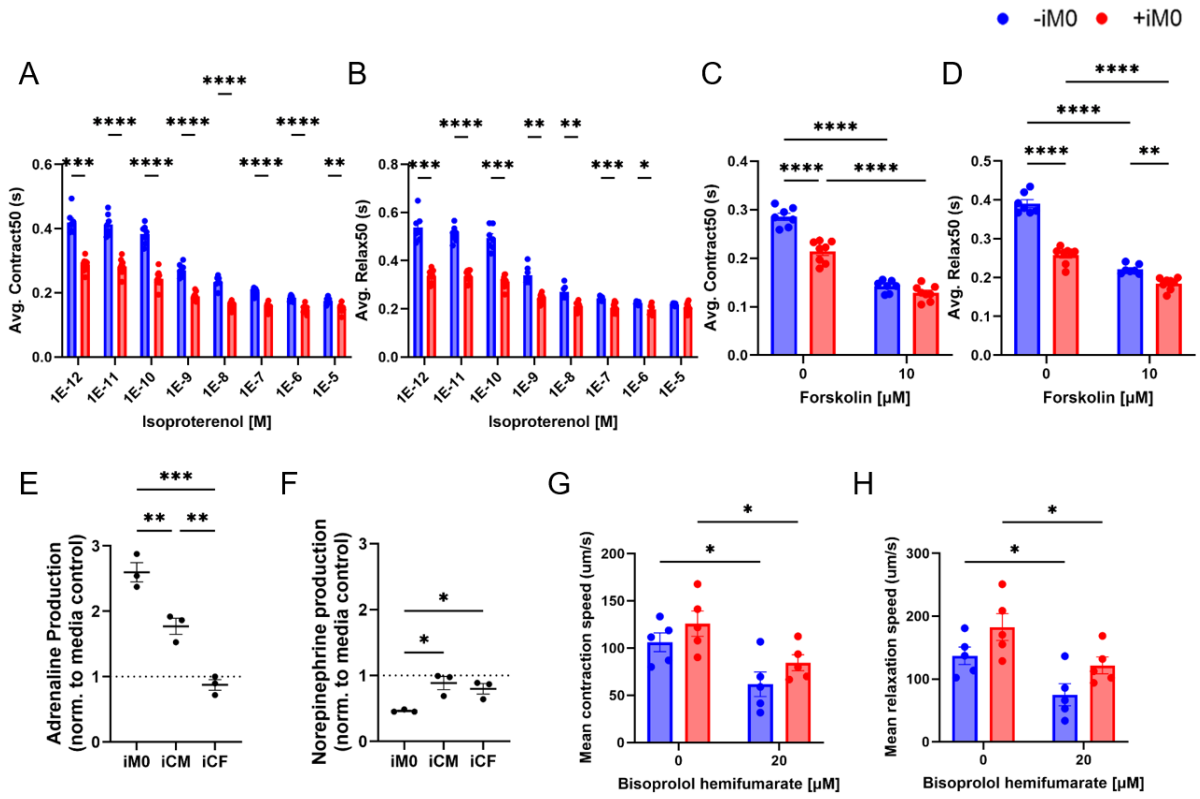

Fig. S5. Supporting data for macrophage modulation of β-adrenergic signaling, Related to Figure 5. (A) Average contract50 (period of time taken from 50% intensity to full peak intensity value during release of calcium) and **(B)** average relax50 (period of time taken from full peak to 50% intensity value during reuptake of calcium) of hECT calcium transients in response to Isoproterenol treatment. **(C)** Average contract50 and **(B)** Average relax50 of hECT calcium transients in response to Forskolin treatment. **(E)** Adrenaline and **(F)** Norepinephrine production by iM0, iCM, and iCF cell populations in 2D monoculture. Statistical significance determined by one-way ANOVA with Tukey's postdoc analysis. **(G)** Mean contraction speed and **(H)** mean relaxation speed of tissue contraction in response to treatment with β1-adrenergic receptor blocker Bisoprolol hemifumarate. Statistical significance was determined by repeated-measures two-way ANOVA with multiple comparisons between groups. All data represent mean ± SEM. *p<0.05, **p<0.01, ***p<0.001, **** p<0.0001.

Target	Oligo Sequence 5’ to 3’
β-Actin Fw	CACCATTGGCAATGAGCGGTTC
β-Actin Rev	AGGTCTTTGCGGATGTCCACGT
CD68 Fw	GAAACGTCACAGTTCATCCAACA
CD68 Rev	ACGTGTAGTCTCCAATGGTCTC
DDR2 Fw	TGTGCACCCCTGGATGAAAC
DDR2 Rev	GTCCTGGGAGGCATATCAAC
GAPDH Fw	AAGGTGAAGGTCGGAGTCAAC
GAPDH Rev	GGGGTCATTGATGGCAACAATA
GATA4 Fw	CCTGAAGCTCTCCCCACAAG
GATA4 Rev	GTCTGTGGAGACTGGCTGAC
TBX20 Fw	ACAGCCTCATTGCTCAACCT
TBX20 Rev	GGCTCTCCACACTTTCCCTC
TCF21 Fw	CAACCTGACGTGGCCCTTTATG
TCF21 Rev	GGAAGCAGAGACAGAGAGCAC
Vimentin Fw	CGGGAGAAATTGCAGGAGGA
Vimentin Rev	AAGGTCAAGACGTGCCAGAG
YFP Fw	GAATACCCCCATCGGCGGCG
YFP Rev	CTCCAGGGCACGGGCACATC

Table S1. Oligo sequences for RT-qPCR, Related to STAR Methods.